

Hole doping and superconductivity characteristics of the $s = 1, 2$ and 3 members of the (Cu,Mo)-12 s 2 homologous series of layered copper oxides

M. Karppinen^{a,*}, Y. Morita^a, T. Kobayashi^a, I. Grigoraviciute^a, J.M. Chen^b,
R.S. Liu^c, H. Yamauchi^a

^aMaterials and Structures Laboratory, Tokyo Institute of Technology, 4259 Nagatsuta, Midori-ku, Yokohama 226-8503, Japan

^bNational Synchrotron Radiation Research Center (NSRRC), Hsinchu, Taiwan, ROC

^cDepartment of Chemistry, National Taiwan University, Taipei, Taiwan, ROC

Received 25 May 2005; received in revised form 4 August 2005; accepted 28 August 2005

Available online 10 October 2005

Abstract

Superconductivity characteristics have been systematically evaluated for a two-CuO₂-plane copper oxide system, (Cu,Mo)-12 s 2, upon increasing the number of fluorite-structured layers, s , between the two CuO₂ planes. Essentially single-phase samples of (Cu_{0.75}Mo_{0.25})Sr₂YCu₂O_{7+ δ} ($s = 1$), (Cu_{0.75}Mo_{0.25})Sr₂(Ce_{0.45}Y_{0.55})₂Cu₂O_{9+ δ} ($s = 2$) and (Cu_{0.75}Mo_{0.25})Sr₂(Ce_{0.67}Y_{0.33})₃Cu₂O_{11+ δ} ($s = 3$) were synthesized through a conventional solid-state route in air. To make the samples superconductive an additional high-pressure oxygenation (HPO) treatment was required. Such treatment (carried out at 5 GPa and 500 °C in the presence of 75 mol% Ag₂O₂ as an oxygen source to maximize the T_c) compressed the crystal lattice for the three members of the (Cu_{0.75}Mo_{0.25})-12 s 2 series equally, i.e., by 0.01 Å for the a parameter and by 0.07 Å for the c parameter per formula unit. From both Cu L -edge and O K -edge XANES spectra the $s = 1$ sample was found to possess the highest overall hole-doping level among the HPO samples. Accordingly it exhibited the best superconductivity characteristics. With increasing s , both the T_c ($s = 1$: 88 K, $s = 2$: 61 K, $s = 3$: 53 K) and H_{irr} values got depressed, being well explained by the trend of decreasing CuO₂-plane hole concentration with increasing s as revealed from O K -edge XANES spectra for the same samples. Hence, the present results do not suggest any significant (negative) impact on the superconductivity characteristics from the gradually thickened fluorite-structured block itself.

© 2005 Elsevier Inc. All rights reserved.

Keywords: High- T_c superconductive copper oxides; Fluorite-structured layers; Homologous series; Oxygen content; Cu valence; XANES spectroscopy

1. Introduction

The crystal structure of a high- T_c superconductive copper oxide is composed of an ordered stack of superconductive CuO₂ plane(s) and nonsuperconductive layers of various types. The nonsuperconductive layers not only provide the (proper) spacing between the CuO₂ planes but also control the hole-doping level of the planes. Here an interesting group of phases is recognized, having two distinct blocks of piled nonsuperconductive layers. One of the blocks is the conventional “blocking block” of rock-

salt (RS) and/or perovskite (P) structured layers, i.e. [AO]_{RS}-[(MO_{1± δ /m})_m]_{P/RS}-[AO]_{RS} where $A = \text{Ba, Sr, etc.}$ and $M = \text{Cu, Bi, Pb, Tl, Hg, etc.}$ This block is glued through the AO layer to a CuO₂ plane by sharing the apical oxygen atom of the CuO₅ pyramid that constitutes the CuO₂ plane. The other layer-piling block of (Ce, R)-[O₂-(Ce, R)] _{$s-1$} ($R = \text{rare earth element}$) in which the valence states of Ce^{IV} and R^{III} are assumed is of the fluorite (F) structure, being inserted between the basal CuO₂ planes of the pyramids. The phase that contains both the two types of blocking block repeats the layer sequence of [AO]_{RS}-[(MO_{1± δ /m})_m]_{P/RS}-[AO]_{RS}-[CuO₂]_P-[(Ce, R)-{O₂-(Ce, R)}] _{$s-1$}]-F-[CuO₂]_P and accordingly obeys a general formula of $M_m A_2 (\text{Ce}, R)_s \text{Cu}_2 \text{O}_{m+4+2s+\delta}$ expressed as $M_m A_2^{(A)} 2s_2$ in

*Corresponding author. Fax: +81 45 924 5365.

E-mail address: karppinen@msl.titech.ac.jp (M. Karppinen).

short [1]. Such phases with F-structured layers are classified as “Category-B” phases, whereas the more common phases with a single nonsuperconductive block only and a general formula of $M_m A_2(\text{Ca}, \text{R})_{n-1} \text{Cu}_n \text{O}_{m+2+2n \pm \delta}$ [$M-m^{(A)}(n-1)n$] belong to “Category-A” [2].

For Category-A phases, a widely adopted practice [1,3–6] has been to discuss both the chemical (oxygen content, hole doping, etc.) and superconductivity (T_c and H_{irr}) characteristics in terms of the number of consecutively stacked CuO_2 planes within one “homologous series”, i.e., a group of phases for which the $[\text{AO}]_{\text{RS}}-[(\text{MO}_{1 \pm \delta/m})_m]_{\text{P}}/\text{RS}-[\text{AO}]_{\text{RS}}$ block is common but the number, n , of the CuO_2 planes in the superconductive $[\text{CuO}_2-\{(\text{Ca}, \text{R})-\text{CuO}_2\}_{n-1}]_{\text{P}}$ block varies [7]. For instance, it has been empirically well established that for each homologous series of Category-A, the highest T_c achieved is due to the $n = 3$ member [1]. Here an interesting question arises, concerning possible systematics among the Category-B phases. Note that for an $M-m^{(A)}2s2$ (M , m and A are fixed) homologous series of Category-B, the members differ from each other in terms of the number of the F-structured cation layers, i.e., s [1,8]. Despite the potential interest, systematic studies on Category-B phases have been rather rare, one of the most apparent reasons being the fact that superconductivity—for a long time—could not be induced into phases with $s \geq 3$ [9–12].

Recently we synthesized a three-fluorite-layer phase of $(\text{Cu}, \text{Mo})-1^{(\text{Sr})232}$ with the composition of $(\text{Cu}_{0.75}\text{Mo}_{0.25})\text{Sr}_2(\text{Ce}_{0.67}\text{Y}_{0.33})_3\text{Cu}_2\text{O}_{11+\delta}$ [13]. Samples synthesized in air did not superconduct, but superconductivity was successfully induced in the as-synthesized samples by means of high-pressure oxygenation. Here we recognize that together with the two earlier established phases, $(\text{Cu}, \text{Mo})-1^{(\text{Sr})212}$ and $(\text{Cu}, \text{Mo})-1^{(\text{Sr})222}$ [14], this $s = 3$ phase forms a homologous series of $(\text{Cu}, \text{Mo})-1^{(\text{Sr})2s2}$ of Category-B. With the parameter s increasing from 1 to 3 the members of the $(\text{Cu}, \text{Mo})-1^{(\text{Sr})2s2}$ series have adjacent two CuO_2 planes separated from each other by a single Y-cation layer for $s = 1$, a “double-fluorite-layer” block of $(\text{Ce}, \text{Y})-\text{O}_2-(\text{Ce}, \text{Y})$ for $s = 2$, and a “triple-fluorite-layer” block of $(\text{Ce}, \text{Y})-\text{O}_2-(\text{Ce}, \text{Y})-\text{O}_2-(\text{Ce}, \text{Y})$ for $s = 3$; for the schematic crystal structures, see Fig. 1. In the present contribution, we present our systematic characterization results for these

three phases in terms of both the doping state of the phase and the superconductivity parameters, T_c and H_{irr} .

2. Experimental

Polycrystalline samples of $(\text{Cu}_{0.75}\text{Mo}_{0.25})\text{Sr}_2\text{YCu}_2\text{O}_{7+\delta}$ ($s = 1$), $(\text{Cu}_{0.75}\text{Mo}_{0.25})\text{Sr}_2(\text{Ce}_{0.45}\text{Y}_{0.55})_2\text{Cu}_2\text{O}_{9+\delta}$ ($s = 2$) and $(\text{Cu}_{0.75}\text{Mo}_{0.25})\text{Sr}_2(\text{Ce}_{0.67}\text{Y}_{0.33})_3\text{Cu}_2\text{O}_{11+\delta}$ ($s = 3$) were synthesized through a solid-state reaction route from appropriate mixtures of high-purity powders of CuO , MoO_3 , SrCO_3 , CeO_2 , and Y_2O_3 . The mixed powders were calcined at 950°C and sintered at 1020°C in air with several intermediate grindings. Portions of these as-air-synthesized (AS) samples were then high-pressure oxygenated (HPO) at 5 GPa and 500°C for 30 min in a cubic-anvil-type high-pressure apparatus in the presence of 75 mol% Ag_2O_2 (against $(\text{Cu}, \text{Mo})-1^{(\text{Sr})2s2}$ formula unit) as an excess-oxygen source [13]. It should be noted that from preliminary experiments we had confirmed that for all the three phases the lattice parameters decreased and the values of T_c and $V(\text{Cu})$ (= average valence of copper) increased with increasing amount of Ag_2O_2 only up to 50–75 mol% of Ag_2O_2 , and then levelled off. Hence, our HPO samples (that are either underdoped or optimally doped but not overdoped) exhibit the highest T_c values achieved for the three phases so far. Also confirmed was from SEM–EDX analysis (for $s = 3$) that the Mo content in a sample that had undergone all the heat-treatment steps yet agreed well with the nominal value. (This was considered important, since MoO_3 is prone to evaporation.)

The samples were characterized by powder X-ray diffraction (XRD; Rigaku: RINT2550VK/U; $\text{Cu } K_\alpha$ radiation) for phase purity and lattice parameters. Oxygen content of the AS $(\text{Cu}, \text{Mo})-1^{(\text{Sr})212}$ ($s = 1$) sample was analyzed by means of iodometric titration, whereas for the other AS samples of the $s = 2$ and 3 phases oxygen-content analysis was not possible by the presently employed standard iodometric titration technique, since the samples did not dissolve in 1 M HCl solution. In the case of the HPO samples, titration experiments were not even tried due to the presence of Ag and/or Ag_2O (originating from Ag_2O_2) in these samples.

For the estimation of the average valence state of copper X-ray absorption near-edge structure (XANES) spectra were collected for the samples at the $\text{Cu } L_{2,3}$ edge. Additionally for the HPO samples O K -edge XANES spectra were collected for the layer-specific hole concentrations. The XANES experiments were performed at the 6-m HSGM beam-line of NSRRC in Hsinchu (Taiwan) in X-ray fluorescence-yield mode; experimental details were as previously given elsewhere [15].

Superconductivity/magnetic properties were measured for all the samples down to 4 K in both field-cooled (FC) and zero-field-cooled (ZFC) modes using a superconducting-quantum-interference-device (SQUID) magnetometer (Quantum Design: MPMS-XL) under 10 Oe. The value of

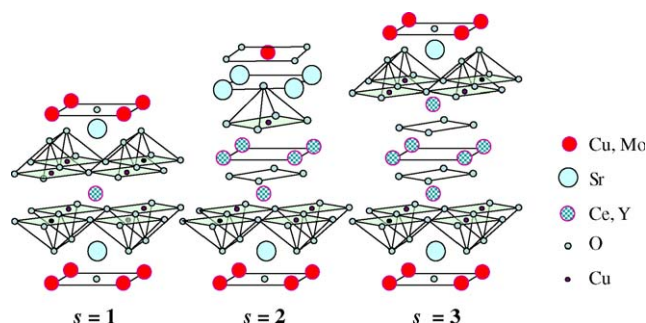


Fig. 1. Schematic presentation of the crystal structures of the first three members of the homologous series, $(\text{Cu}, \text{Mo})-1^{(\text{Sr})2s2}$.

T_c was defined at the onset temperature of the diamagnetic signal. For the superconductive samples the $H_{irr}(T)$ characteristics were evaluated using the procedure introduced elsewhere [16]. In brief, the magnetic field (H) dependence of critical current $J_c(H)$ was calculated via Bean's model from the measured magnetization (M) vs. H hysteresis loops, and then the H_{irr} value was determined from the $\log(H)$ vs. $J_c(H)$ plot as the H value at the limit of $J_c \rightarrow 0$.

3. Results and discussion

From X-ray diffraction patterns shown for all the six samples in Fig. 2, all the three AS samples are found to be essentially free from impurity phases (except the trace of CeO_2 seen for the $s = 3$ sample), whereas the corresponding HPO samples naturally contain Ag and/or Ag_2O as residues from Ag_2O_2 used as the excess oxygen source. Lattice-parameter refinements were carried out in tetragonal space groups, $P4/mmm$ ($s = 1$ and 3) and $I4/mmm$ ($s = 2$) [12,13]. In the former/latter case the unit cell contains one/two formula units along the c -axis, ref. Fig. 1. In Table 1, we give—for the sake of an easier comparison—the lattice parameters for all the three phases per one

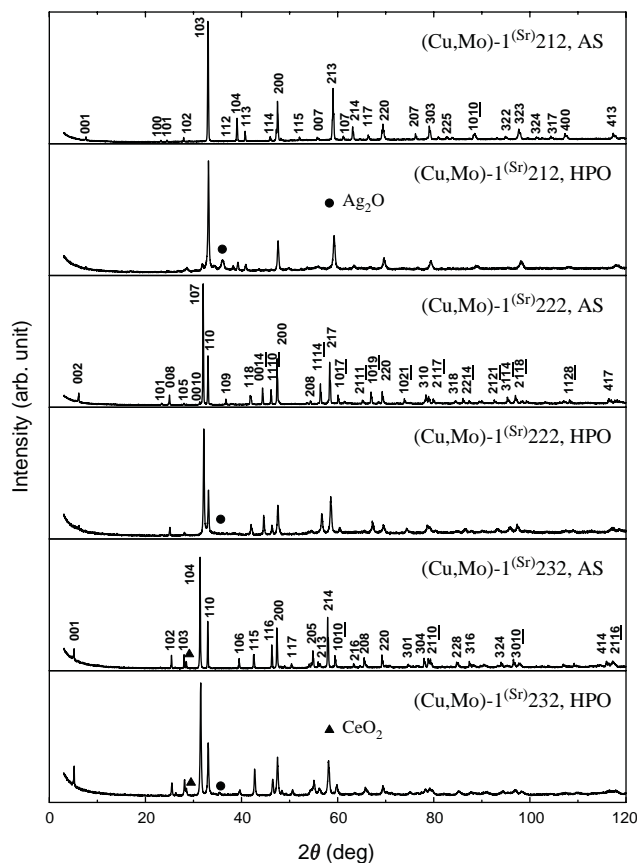


Fig. 2. X-ray diffraction patterns for the AS (as-synthesized) and HPO (high-pressure oxygenated) samples of $(\text{Cu},\text{Mo})-1(\text{Sr})_{2s}2$: $(\text{Cu}_{0.75}\text{Mo}_{0.25})\text{Sr}_2\text{YCu}_2\text{O}_{7+\delta}$ ($s = 1$), $(\text{Cu}_{0.75}\text{Mo}_{0.25})\text{Sr}_2(\text{Ce}_{0.45}\text{Y}_{0.55})_2\text{Cu}_2\text{O}_{9+\delta}$ ($s = 2$) and $(\text{Cu}_{0.75}\text{Mo}_{0.25})\text{Sr}_2(\text{Ce}_{0.67}\text{Y}_{0.33})_3\text{Cu}_2\text{O}_{11+\delta}$ ($s = 3$). (Indexing within the $P4/mmm$ space group for $s = 1$ and 3, and $I4/mmm$ for $s = 2$.)

formula unit. High-pressure oxygenation apparently compresses the lattice for all the three phases (as expected for a layered copper oxide upon increasing oxygen content). Interestingly, the magnitude of lattice-parameter contraction is exactly of the same magnitude for the three members of the $(\text{Cu},\text{Mo})-1(\text{Sr})_{2s}2$ series, i.e., 0.01 \AA for the a parameter and 0.07 \AA for the c parameter (per formula unit). Another interesting point to observe from Table 1 is that the a lattice parameter is clearly shorter for the $s = 1$ phase than for the higher homologues of the series. This trend applies to both AS and HPO samples, and suggests that the $s = 1$ phase is more strongly doped with holes than the other two phases.

To gain quantitative data on the doping state of the three phases, we characterized the samples (both AS and HPO) for the average (over the two Cu lattice sites) valence of copper, $V(\text{Cu})$, on the basis of Cu $L_{2,3}$ -edge XANES spectroscopy. Obtained spectra are shown in Fig. 3. The L_{3} -edge area from 925 to 940 eV was used for the evaluation of $V(\text{Cu})$: the main peak at around 931.2 eV is due to divalent copper states (Cu^{II} : $3d^9$), whereas the high-energy shoulder about 932.8 eV originates from trivalent copper (Cu^{III} : $3d^8L$, where $L = \text{oxygen-ligand hole}$) [17]. From Fig. 3, as expected, the high-energy shoulder due to Cu^{III} significantly enhances for all the three $(\text{Cu},\text{Mo})-1(\text{Sr})_{2s}2$ phases upon HPO. Details of the spectral features were analyzed following Ref. [18]. In short, the two L_{3} -edge peaks about 931.2 and 932.8 eV were fitted with Gaussian functions after approximating the background to a straight line, and from the obtained integrated intensities of the peaks, i.e., $I(\text{Cu}^{\text{II}})$ and $I(\text{Cu}^{\text{III}})$, respectively, $V(\text{Cu})$ was calculated as $V(\text{Cu}) \equiv 2 + I(\text{Cu}^{\text{III}})/[I(\text{Cu}^{\text{II}}) + I(\text{Cu}^{\text{III}})]$. It should be noted that the resultant absolute values for $V(\text{Cu})$ (given in Table 1), may somewhat (± 0.03) deviate from the true Cu valence values, since the raw absorption data were not corrected for the self-absorption effect [19]. Nevertheless, our $V(\text{Cu})$ values should be reliable enough in detecting relative changes or differences in the average valence state of copper. From Table 1, $V(\text{Cu})$ values for the HPO samples are higher by 0.15–0.25 in comparison to those for the corresponding AS samples. This is compatible with an increase in the oxygen content of the phase upon HPO by 0.20–0.35 oxygen atoms per formula unit, if one assumes that the valences of the other constituent cations remain unchanged upon HPO. Our preliminary TG analysis for the HPO samples of the $(\text{Cu},\text{Mo})-1(\text{Sr})_{232}$ phase, however, suggested that the amount of oxygen incorporated upon HPO would be of the level of 0.5 oxygen atoms per formula unit [13]. Hence, it is possible that besides Cu also other constituent element(s) (presumably Mo) are oxidized as well. From the $V(\text{Cu})$ values we may also calculate the largest possible oxygen content for each sample that would yet be compatible with the $V(\text{Cu})$ value by setting the valence values of the other cations to their maximum values, i.e., Mo^{VI} , Sr^{II} , Ce^{IV} and Y^{III} . The resultant δ_{max} values are given in Table 1. It is seen that for all the samples the oxygen content, $1 + \delta$, of

Table 1

Characterization results for the (Cu,Mo)-1(Sr)_{2s}2 samples: lattice parameters, a and c , and the values of superconductivity transition temperature, T_c , average Cu valence, $V(\text{Cu})$ (from Cu $L_{2,3}$ -edge XANES data), and “largest possible” oxygen content, δ_{max} (calculated from the $V(\text{Cu})$ value by setting the valence values of the other cations to their maximum values, i.e., Mo^{VI}, Sr^{II}, Ce^{IV} and Y^{III}), and peak intensities, I_{CR} and I_{CuO_2} (of the 527.5 eV and 528.2 eV pre-edge peaks in the O K -edge XANES spectra; see the text). Note that even though the absolute values of I_{CR} and I_{CuO_2} do not have any meaning, their relative values are supposed to be proportional to the hole concentrations in the (Cu,Mo)O_{1+ δ} charge reservoir and in the CuO₂ plane, respectively. Then, the sum, $I_{\text{CR}} + 2I_{\text{CuO}_2}$, provides us with a measure for the overall hole concentration of the phase

Sample	Lattice parameter (Å)		T_c (K)	$V(\text{Cu})$	δ_{max}	I_{CR}	I_{CuO_2}	$I_{\text{CR}} + 2I_{\text{CuO}_2}$
	a	c						
$s = 1$: AS	3.825(1)	11.54(1)	<4	2.19(4)	0.3(1)			
$s = 1$: HPO	3.815(1)	11.47(1)	88	2.45(4)	0.6(1)	0.21(3)	0.20(3)	0.61(5)
$s = 2$: AS	3.832(1)	14.27(1) ^a	<4	2.12(4)	0.1(1)			
$s = 2$: HPO	3.822(1)	14.20(1) ^a	61	2.26(4)	0.3(1)	0.11(3)	0.16(3)	0.43(5)
$s = 3$: AS	3.836(1)	16.99(1)	<4	2.12(4)	0.2(1)			
$s = 3$: HPO	3.828(1)	16.92(1)	53	2.28(4)	0.4(1)	0.15(3)	0.08(3)	0.31(5)

^a $c/2$.

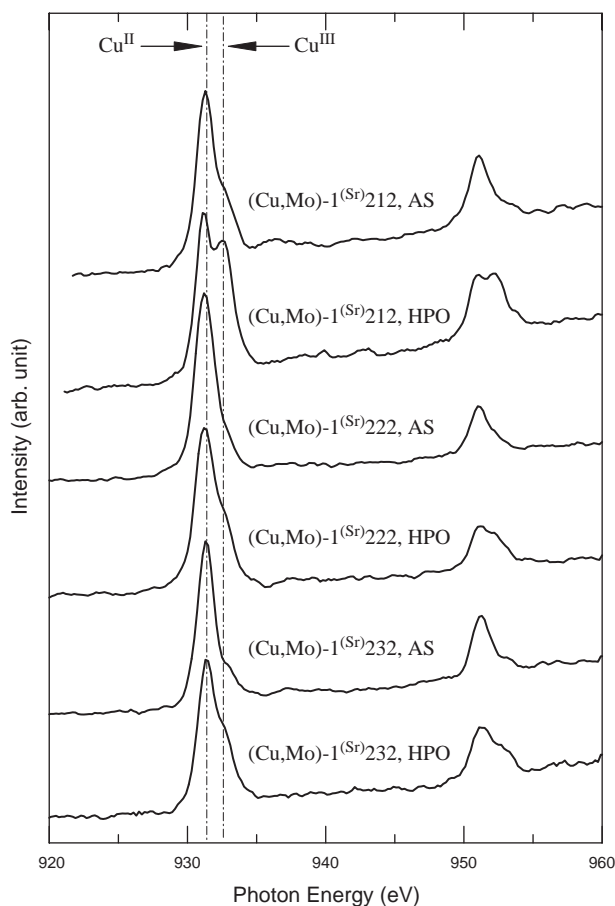


Fig. 3. Cu $L_{2,3}$ -edge XANES spectra for the (Cu,Mo)-1(Sr)_{2s}2 samples (AS and HPO).

the (Cu_{0.75}Mo_{0.25})O_{1+ δ} charge reservoir remains lower than 2, i.e., around 1.1–1.3 for the AS samples and 1.3–1.6 for the HPO samples. For the AS (Cu,Mo)-1(Sr)²¹² ($s = 1$) sample the absolute oxygen content was successfully established by means of iodometric titration: the result was $\delta = 0.21(2)$, whereas δ_{max} was calculated at 0.3(1) (Table 1). We thus tentatively propose that in the AS samples Mo is in a valence state somewhat lower than VI,

but is then most likely oxidized together with Cu upon the HPO treatment.

Magnetic susceptibility data for the samples are given in Fig. 4. None of the AS samples show superconductivity, whereas all the three HPO samples are bulk superconductors (volume fraction higher than 30%). The T_c values are listed in Table 1. With increasing s , T_c decreases from 88 K for $s = 1$ to 61 K for $s = 2$ and 53 K for $s = 3$. From Table 1, it is seen that among the three HPO samples, the $s = 1$ sample that shows the highest T_c also possesses the largest $V(\text{Cu})$ value. For the $s = 2$ and 3 phases, the $V(\text{Cu})$ value is essentially the same, but the $s = 3$ phase possesses lower T_c than the $s = 2$ phase. A plausible explanation is found from the O K -edge XANES data.

Fig. 5 displays the very pre-edge (524–536 eV) area of the O K -edge XANES spectra of the HPO samples. For all the three samples, three partly overlapping peaks are distinguished within 526–532 eV. Following the interpretation established for CuBa₂YCu₂O_{7- δ} (Cu-1^(Ba)212 or “Y-123”) [17], we assign the lowest-energy peak at around 527.5 eV to the oxygen hole states in the (Cu,Mo)O_{1+ δ} charge reservoir (CR) and the peak at around 528.2 eV to the oxygen hole states in the CuO₂ plane. The latter spectral feature is common to all the p-type doped superconductive copper oxides [15,17,18]. The peak about 530.0 eV arises from a transition into O2p states hybridized with the upper Hubbard band (UHB). The spectral features within 526–532 eV were analyzed by fitting Gaussian functions to the three peaks. Before the fitting, each spectrum was normalized to have the same intensity for the main peak in the energy range of 522–560 eV. Furthermore, after the fitting the integrated intensities of the peaks were multiplied by the nominal oxygen content of the sample, i.e., 7.6 for $s = 1$, 9.3 for $s = 2$ and 11.4 for $s = 3$ (ref. δ_{max} values in Table 1). The thus obtained intensities, given in Table 1, for the 527.5-eV (I_{CR}) and 528.2-eV ($I_{2 \times \text{CuO}_2} = 2I_{\text{CuO}_2}$) peaks are supposed to reflect the hole concentrations in the (Cu,Mo)O_{1+ δ} charge reservoir and the two CuO₂ planes of the unit cell, respectively, though the absolute values as

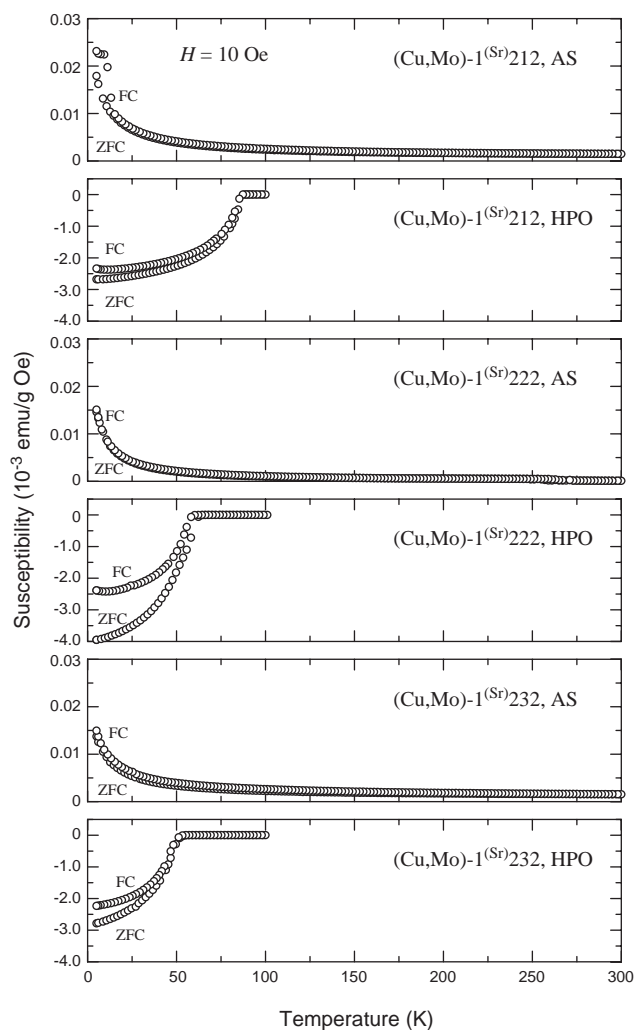


Fig. 4. Temperature dependence of magnetic susceptibility for the $(\text{Cu,Mo})\text{-}1^{(\text{Sr})}2s2$ samples (AS and HPO).

such have no meaning. Nevertheless, relative comparison is possible among the three $(\text{Cu,Mo})\text{-}1^{(\text{Sr})}2s2$ phases. From Table 1, we can first of all see that the overall hole-content value, $I_{\text{CR}} + 2I_{\text{CuO}_2}$, correlates reasonably well with the value of $V(\text{Cu})$ from the Cu L -edge XANES data. From both $I_{\text{CR}} + 2I_{\text{CuO}_2}$ and $V(\text{Cu})$, the $s = 1$ phase is most strongly doped with holes, whereas the higher homologues, $s = 2$ and 3 , are of the same overall doping level (the same was also suspected based on the a lattice parameter values for the three phases). Further comparison between the I_{CR} and I_{CuO_2} values reveals that the holes are distributed differently in the $s = 2$ and 3 phases: in the former the holes are more strongly concentrated in the CuO_2 plane whereas in the latter in the $(\text{Cu,Mo})\text{O}_{1+\delta}$ charge reservoir [20]. From Table 1, the differences in the T_c values among the three $(\text{Cu,Mo})\text{-}1^{(\text{Sr})}2s2$ phases (HPO samples) follow well the differences in the actual hole-doping level of the CuO_2 plane, i.e., the I_{CuO_2} value.

Fig. 6 displays the $H_{\text{irr}}(T)$ lines against the reduced temperature, $1 - T/T_c$, for the superconductive HPO

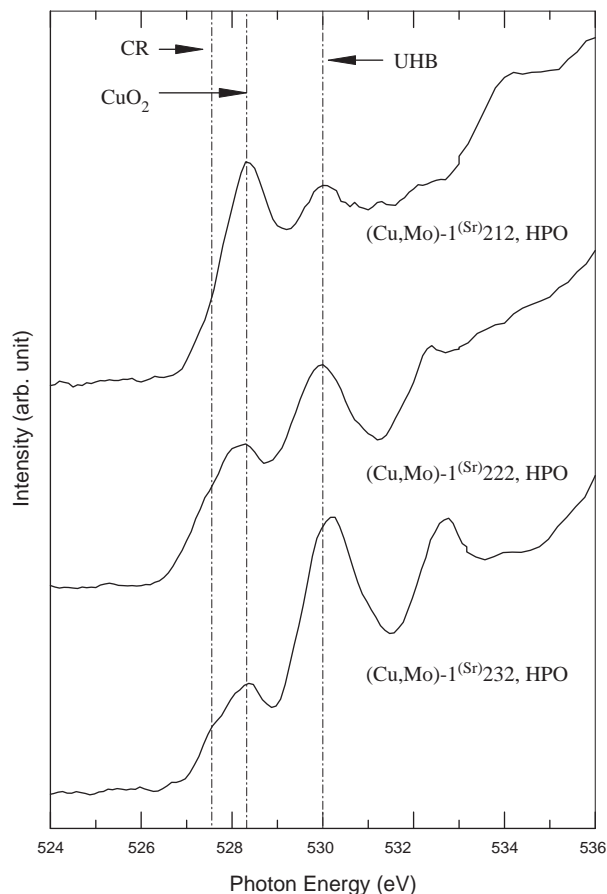


Fig. 5. O K -edge XANES spectra for the HPO samples of $(\text{Cu,Mo})\text{-}1^{(\text{Sr})}2s2$.

samples. Also included are data for a $\text{CuBa}_2\text{YCu}_2\text{O}_{6.93}$ or $\text{Cu-}1^{(\text{Ba})}212$ sample ($T_c = 93$ K, $V(\text{Cu}) = 2.28$) from Ref. [21]. In general, the $H_{\text{irr}}(T)$ lines of high- T_c superconductive copper oxides are controlled by both intrinsic and extrinsic flux pinning properties. Here, among our similarly synthesized samples of the same homologous series, we believe that the possible differences in the $H_{\text{irr}}(T)$ characteristics should originate from differences in the intrinsic pinning properties among these samples. For Category-A phases, the intrinsic $H_{\text{irr}}(T)$ characteristics are enhanced [3,16]: (i) by increasing the overall concentration of (mobile) holes [22,23] and/or (ii) by optimizing their distribution between the superconductive and the blocking blocks [24] (to enhance the thermodynamical stability of magnetic fluxons in the superconductive $\text{CuO}_2\text{-}(\text{Q-CuO}_2)_{n-1}$ block), and (iii) by enhancing the conductivity [25–27] and/or (iv) by decreasing the thickness [27–30] of the $\text{AO-}(\text{MO}_{1\pm\delta/m})_m\text{-AO}$ blocking block (to improve the correlation of fluxons between two adjacent superconductive blocks through the blocking block). In comparison to the $\text{Cu-}1^{(\text{Ba})}212$ reference sample, the $H_{\text{irr}}(T)$ line of the present $(\text{Cu,Mo})\text{-}1^{(\text{Sr})}212$ sample is located at significantly lower fields, even though the average valence of copper is higher for the latter sample. This could be due a decrease in

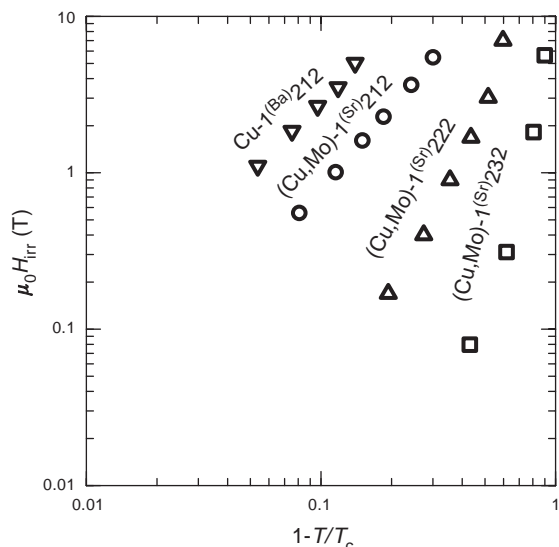


Fig. 6. $H_{\text{irr}}(T)$ lines for the high-pressure oxygenated (HPO) samples of $(\text{Cu},\text{Mo})\text{-}1^{(\text{Sr})}2s2$. The data for the $\text{Cu-}1^{(\text{Ba})}212$ ($\text{CuBa}_2\text{YCu}_2\text{O}_{6.93}$) sample [21] are given for reference.

the concentration of mobile holes within the $(\text{Ba},\text{Sr})\text{O}-(\text{Cu},\text{Mo})\text{O}_{1+\delta}$ blocking block that most likely takes place as the conductive $\text{CuO}_{1+\delta}$ chains get broken as a consequence of the Sr-for-Ba [31] and Mo-for-Cu substitutions. Note that even the former substitution alone is known to deteriorate the $H_{\text{irr}}(T)$ characteristics of the $\text{Cu-}1^{(\text{Ba},\text{Sr})}212$ phase [31,32]. Then, among the $(\text{Cu},\text{Mo})\text{-}1^{(\text{Sr})}2s2$ samples, the $H_{\text{irr}}(T)$ characteristics are depressed with increasing s (Fig. 6). This is well explained by the fact that the CuO_2 -plane hole concentration decreases with increasing s (viz. I_{CuO_2} in Table 1). Therefore, it seems that no additional (negative) contribution from the gradually thickened fluorite-structured block between the superconductive CuO_2 planes is evident from the present data.

4. Conclusion

Our systematic study on the first three members of the $(\text{Cu}_{0.75}\text{Mo}_{0.25})\text{-}1^{(\text{Sr})}2s2$ homologous series has shown that increasing the number of fluorite-structured layers, s , between the two CuO_2 planes makes it increasingly difficult to oxygenate the phase. Therefore the higher- s members remain underdoped and accordingly the T_c and H_{irr} values lower. The observed superconductivity characteristics are well explained by the differences in the overall hole-doping level/ CuO_2 -plane hole concentration revealed from the Cu L -edge and O K -edge XANES data. Hence, we suggest that the increasing separation of superconductive CuO_2 planes does not itself have any significant effect on the superconductivity characteristics of multi-layered copper oxides.

Acknowledgment

This work was supported by Grants-in-aid for Scientific Research (Nos. 15206002 and 15206071) from the Japan Society for the Promotion of Science.

References

- [1] M. Karppinen, H. Yamauchi, Mater. Sci. Eng. R 26 (1999) 844.
- [2] T. Wada, A. Ichinose, H. Yamauchi, S. Tanaka, J. Ceram. Soc. Jpn. Int. Ed. 99 (1991) 420.
- [3] J.L. Tallon, R.G. Buckley, P.W. Gilberd, M.R. Presland, I.W.M. Brown, M.E. Bowden, L.A. Christian, R. Goguel, Nature 333 (1988) 153; R.G. Buckley, J.L. Tallon, I.W.M. Brown, M.R. Presland, N.E. Flower, P.W. Gilberd, M. Bowden, N.B. Milestone, Physica C 156 (1988) 629.
- [4] S.S.P. Parkin, V.Y. Lee, A.I. Nazzal, R. Savoy, R. Beyers, S.J. La Place, Phys. Rev. Lett. 61 (1988) 750.
- [5] M. Marezio, E.V. Antipov, J.J. Capponi, C. Chaillout, S. Loureiro, S.N. Putilin, A. Santoro, J.L. Tholence, Physica B 197 (1994) 570; J.J. Capponi, J.L. Tholence, C. Chaillout, M. Marezio, P. Bordet, J. Chenavas, S.M. Loureiro, E.V. Antipov, E. Kopnine, M.F. Gorius, M. Nunez-Regueiro, B. Souletie, P. Radaelli, F. Gerhards, Physica C 235–240 (1994) 146.
- [6] S.M. Loureiro, Y. Matsui, E. Takayama-Muromachi, Physica C 302 (1998) 244.
- [7] H. Yamauchi, M. Karppinen, S. Tanaka, Physica C 263 (1996) 146.
- [8] For Category-B phases the number of CuO_2 planes per formula unit is fixed at 2. Hence, an $M\text{-}m^{(A)}2s2$ phase at $s = 1$ (Category-B) also belongs to Category-A, i.e., $M\text{-}m^{(A)}2(n-1)n$ at $n = 2$.
- [9] T. Wada, A. Ichinose, H. Yamauchi, S. Tanaka, Physica C 171 (1990) 344; T. Wada, A. Ichinose, F. Izumi, A. Nara, H. Yamauchi, H. Asano, S. Tanaka, Physica C 179 (1991) 455; H.W. Zandbergen, T. Wada, A. Nara, H. Yamauchi, S. Tanaka, Physica C 183 (1991) 149.
- [10] A. Tokiwa, T. Oku, M. Nagoshi, Y. Syono, Physica C 181 (1991) 311.
- [11] S. Ikegawa, Y. Motoi, Appl. Phys. Lett. 68 (1996) 2430; S. Ikegawa, K. Nakayama, Y. Motoi, M. Arai, Phys. Rev. B 66 (2002) 14536; S. Ikegawa, K. Nakayama, M. Arai, Physica C 384 (2003) 61.
- [12] M. Karppinen, V.P.S. Awana, Y. Morita, H. Yamauchi, Physica C 392–396 (2003) 82.
- [13] Y. Morita, T. Nagai, Y. Matsui, H. Yamauchi, M. Karppinen, Phys. Rev. B 70 (2004) 174515.
- [14] A. Ono, Jpn. J. Appl. Phys. 32 (1993) 4517.
- [15] J.M. Chen, R.S. Liu, W.Y. Liang, Phys. Rev. B 54 (1996) 12587.
- [16] H. Yamauchi, M. Karppinen, K. Fujinami, T. Ito, H. Suematsu, H. Sakata, K. Matsuura, K. Isawa, Supercond. Sci. Technol. 11 (1998) 1006.
- [17] N. Nücker, E. Pellegrin, P. Schweiss, J. Fink, S.L. Molodtsov, C.T. Simmons, G. Kaindl, W. Frentrup, A. Erb, G. Müller-Vogt, Phys. Rev. B 51 (1995) 8529.
- [18] M. Karppinen, M. Kotiranta, T. Nakane, H. Yamauchi, S.C. Chang, J.M. Chen, R.S. Liu, Phys. Rev. B 67 (2003) 134522.
- [19] It was considered counterproductive to carry out self-absorption correction due to not-well-defined amounts of Ag and Ag_2O in the samples.
- [20] Our observation that among the three $(\text{Cu},\text{Mo})\text{-}1^{(\text{Sr})}2s2$ phases, in $(\text{Cu},\text{Mo})\text{-}1^{(\text{Sr})}222$ the holes are most efficiently concentrated in the CuO_2 plane may have its origin in the fact that in this phase the positive charge of the fluorite-structured $(\text{Ce},\text{Y})\text{-}\{\text{O}_2\text{-}(\text{Ce},\text{Y})\}_{s-1}$ block is the lowest, i.e., 2.9 for $s = 2$ whereas 3.0 for $s = 1$ and 3.

- [21] The Cu-1^(Ba)212 reference sample was synthesized by a conventional solid-state synthesis route, annealed in 1 atm O₂ and characterized for $V(\text{Cu})$, T_c and H_{irr} through procedures equivalent to those used for the (Cu,Mo)-1^(Sr)2s2 samples. The oxygen content was precisely determined by means of iodometric titration.
- [22] K. Kishio, J. Shimoyama, T. Kimura, Y. Kotaka, K. Kitazawa, K. Yamafuji, Q. Li, M. Suenaga, *Physica C* 235–240 (1994) 2775.
- [23] K. Fujinami, H. Suematsu, M. Karppinen, H. Yamauchi, *Physica C* 307 (1998) 202; M. Karppinen, H. Yamauchi, T. Nakane, M. Kotiranta, *Physica C* 338 (2000) 18.
- [24] Y. Yasukawa, T. Nakane, H. Yamauchi, M. Karppinen, *Appl. Phys. Lett.* 78 (2001) 2917; M. Karppinen, N. Kiryakov, Y. Yasukawa, T. Nakane, H. Yamauchi, *Physica C* 382 (2002) 66.
- [25] J.L. Tallon, G.V.M. Williams, C. Bernhard, D.M. Pooke, M.P. Staines, J.D. Johnson, R.H. Meinhold, *Phys. Rev. B* 53 (1996) R11972.
- [26] K. Kishio, J. Shimoyama, A. Yoshikawa, K. Kitazawa, O. Chmaissem, J.D. Jorgensen, *J. Low Temp. Phys.* 105 (1996) 1359.
- [27] J.L. Tallon, G.V.M. Williams, J.W. Loram, *Physica C* 338 (2000) 9.
- [28] J. Shimoyama, S. Hahakura, R. Kobayashi, K. Kitazawa, K. Yamafuji, K. Kishio, *Physica C* 235–240 (1994) 2795.
- [29] V. Hardy, A. Maignan, C. Martin, F. Warmont, J. Provost, *Phys. Rev. B* 56 (1997) 130.
- [30] M.P. Raphael, M.E. Reeves, E.F. Skelton, C. Kendziora, *Phys. Rev. Lett.* 84 (2000) 1587.
- [31] T. Nakane, K. Isawa, R.S. Liu, J.M. Chen, H. Yamauchi, M. Karppinen, *J. Solid State Chem.* 177 (2004) 1925.
- [32] L. Parent, C. Moreau, *J. Mater. Sci.* 26 (1991) 5873.